Int J Clin Exp Pathol 2017;10(7):7498-7510
www.ijcep.com /ISSN:1936-2625/IJCEP0052487

Original Article

Protosappanin a inhibits osteoclastogenesis via reducing oxidative stress in RAW264.7 cells

Qiang Huang*, Rui-Ying Meng*, Yan-Wei Yang*, Meng Li, Fei Wang, Wei-Wei Shen, Xiao-Wen Deng, Shun-Gang Zhou, Yun Xue, Qiu-Ming Gao

*Lanzhou General Hospital of Lanzhou Military Command, Lanzhou, Gansu, People's Republic of China. *Equal contributors.*

Received March 8, 2017; Accepted May 23, 2017; Epub July 1, 2017; Published July 15, 2017

Abstract: Protosappanin A (PrA), obtained from the traditional Chinese herbal medicine, *Caesalpinia sappan L.* (*Lignum Sappan*), possesses a lot of pharmaceutical activities. Typically, it is a potent antioxidant. This study makes an effort to test its protective effects against osteoporosis by partially reducing oxidative stress in RAW264.7 cells and a mouse ovariectomized (OVX) osteoporosis model. The influence that PrA affected on osteoclastic proliferation and differentiation under oxidative status was investigated. Our results revealed that PrA significantly inhibited the proliferation of RAW264.7 cells in oxidative stress conditions. Moreover, it suppressed some osteoclastic markers by TRAP staining, bone section assay and quantitative real-time PCR. PrA decreased reactive oxygen species (ROS) generation in RAW264.7 cells. *In vivo*, our results demonstrated that PrA supplementation improved some serum oxidative markers, including malondialdehyde (MDA) and reduced glutathione (GSH), and inhibited some osteoclastic markers, such as CTX-1 and TRAP. Importantly, it ameliorated the micro-architecture of trabecular bones by micro-CT assay. In summary, these findings showed that protection by PrA against osteoporosis is associated with a reduction in oxidative stress, suggesting that PrA may be useful in bone resorption related diseases, especially osteoporosis.

Keywords: Protosappanin A, osteoclastogenesis, osteoporosis, ovariectomized mouse, reactive oxygen species

Introduction

Osteoporosis is a common disease worldwide and is characterized by decreased bone mineral density (BMD) and progressive destruction of the bone micro-structure, resulting in increased bone fragility and risk of fractures [1]. Oxidative stress is a biochemical disequilibrium propitiated by excessive production of free radicals and ROS, which provoke oxidative damage to bio-molecules and which cannot be counteracted by antioxidative systems [2]. Approximately 3 to 10% of the oxygen utilized by tissues is converted to ROS intermediates, such as free radicals. Free radicals impair cell and tissue function by oxidizing and degrading biologically important molecules, including proteins, lipids and DNA [3]. Based on epidemiological studies in humans and mechanistic studies in animal models, oxidative stress has been shown to be a crucial pathogenic factor of osteoporosis [4]. For example, osteoporotic postmenopausal women display decreased BMD related to a higher oxidation of plasma lipids and lower superoxide dismutase and catalase efficacy [5-7]. In rat femurs, ovariectomy results in oxidative stress and decreases the capacity of antioxidant defense mechanisms [8]. Thus, oxidative stress may serve as a major contributor to postmenopausal osteoporosis [5]. Both aging and estrogen deficiency promote ROS generation, and there is strong evidence to indicate that the damage in bone mass due to estrogen loss may be prevented by antioxidants [9].

Osteoclasts are unique bone resorptive cells that branch from the monocyte or macrophage lineage. These cells are necessary for the maintenance of skeletal homeostasis. A relative excess of their activity, however, often eventuates in the common disorder osteoporosis [10].

Recent *in vitro* studies or animal models have shown that oxidative stress has an important impact on osteoclast differentiation and functions [11, 12]. ROS can improve bone resorption by directly promoting osteoclastic development and activity [13]. Moreover, it has been suggested that ROS produced by osteoclasts stimulate and facilitate resorption of bone tissue under normal physiological conditions [14, 15]. Estrogen deficiency, which occurs after menopause, leads to bone loss through increased osteoclastic function and subsequently represents the major pathological determinant responsible for postmenopausal bone loss because ROS stimulate osteoclasts [16, 17]. Bone turnover changes, including maintenance of or increases in bone resorption and decreases in bone formation, are significantly found in postmenopausal osteoporosis, leading to net bone loss [18].

Bisphosphonates, such as alendronate and risedronate, are the most commonly used drugs in the treatment of osteoporosis. Bisphosphonates, which are inhibitors of bone resorption, can reduce bone resorption and decrease bone turnover [19]. However, many studies have shown that bisphosphonates can result in many side effects, including osteonecrosis, atypical femoral fractures and renal dysfunction [20, 21]. Thus, natural substances that possess antioxidant activity may represent a better method to modulate the activity of osteoclasts in the maintenance of bone structure and volume. PrA, a bio-active compound, is isolated from *Caesalpinia sappan L*. Previous studies have shown that PrA exhibits immuno-suppressive and anti-oxidative properties [22, 23]. In addition, PrA displays inhibitory effects on NO generation and linoleic acid oxidation in the cultured J774.1 (macrophage-like) cell line *in vitro*, and this effect may be due to the suppression of iNOS gene expression by PrA [24]. Ke-Wu Zeng and his colleagues reported that PrA has anti-oxidative/nitrative activities on brain immune and neuro-inflammation through regulation of the CD14/TLR4-dependent IKK/IκB/NF-κB inflammation signal pathway [23].

We are very interested in the effects of PrA in bone resorption. Thus, the objective of this research was to investigate the potential anti-osteoporosis effects of PrA and its underlying mechanisms *in vitro* and *in vivo*.

Methods

Materials

PrA isolated from *Caesalpinia sappan L*. (molecular weight 272.25, purity > 98%, dissolved in distilled water) was purchased from Shanghai Tauto Biotech Co., Ltd. (China). The ROS assay kit and the GSH and MDA assay kits were obtained from the Beyotime Institute of Biotechnology (Shanghai, China). The TRAP assay kit was obtained from Sigma (Sigma-Aldrich, US). The CTX-1 and TRAP ELISA assay kits were obtained from Immune Diagnostic System Inc. (Fountain Hill, AZ, USA). The BrdU incorporation assay kit was obtained from Cell Signaling Technology. All other reagents were of analytical grade.

Cell culture and differentiation

RAW264.7 cells, which belong to a mouse monocyte/macrophage cell line, were cultured in 12-well plates in α-MEM with 10% heat-inactivated FBS, 100 U/ml penicillin and 100 μg/ml streptomycin in 5% CO_2 at 37°C. To induce osteoclastic differentiation, the medium was supplemented with 50 ng/ml RANKL [25]. H_2O_2 served as an exogenous ROS source, and N-acetyl-L-cysteine (NAC) acted as a ROS cleaner. After the cells reached confluence, serum-free medium containing PrA was dissolved in distilled water and added to the cells, and the cells were incubated for 24 h prior to treatment with 300 μM H_2O_2 for 24 h. For each experiment, PrA administration was performed prior to H_2O_2 treatment. All of the experiments were performed in duplicate wells and repeated three times.

MTT assay of cell survival

In this study, RAW264.7 cells were treated with different concentrations of PrA (0, 0.1, 1, and 10 μM) for 24, 48 and 72 h to measure the toxicity of PrA. MTT assays were performed as previously described and were used to assess cell survival [26].

BrdU proliferation assay

Cell proliferation was assayed using a BrdU incorporation assay kit according to the manufacturer's instructions. BrdU was added 12 h before culture termination. At the end of the

culture period, the cells were fixed with fixing solution for 30 min at RT, rinsed twice with PBS, and incubated with monoclonal anti-BrdU antibody for 1 h and then with anti-mouse secondary antibody for 30 min. After washing with PBS, the samples were further stained with DAPI for 5 min and washed three times with PBS. The percentage of BrdU-positive cells was analyzed by randomly counting the positive cells and the total cells from three different fields of vision for each group of cells.

TRAP staining of RAW264.7 cells

After osteoclastic induction for six days, RAW264.7 cells were subjected to a TRAP staining assay using a TRAP assay kit and observed using a microscope. The TRAP-positive multinuclear macrophages with more than three nuclei were counted as osteoclasts. The number of osteoclasts in each well for all of the groups was counted, and the average for each group was calculated.

Staining of bone resorption pits

RAW264.7 cells were plated on bone slices and cultured with RANKL for six days to generate mature osteoclasts. The cells were then removed from the bone slices through mechanical agitation. The bone slices were incubated with peroxidase-conjugated wheat germ agglutinin for 1 h and stained with 3,3'-diaminobenzidine. The entire resorption lacunae was observed and counted under optical microscope. According to the number of resorption pits, we determined the resorption function of osteoclasts. The results were expressed in lacunae number/slice [27].

Quantitative real-time PCR to test osteoclastic differentiation

After osteoclastic induction for six days, RAW264.7 cells were incubated with serum-free medium containing PrA and/or H_2O_2 for two days. The total cellular RNA from these cells was extracted using the Trizol reagent. Single-strand cDNA synthesis was performed using the Prime Script RT reagent kit (TaKaRa). RT-PCR was performed using the CFX96 (BIO-RAD) instrument as previously described [28]. Individual PCRs were performed in 96-well optical reaction plates with SYBR Green-I (TaKaRa) according to the manufacturer's instructions. The expression levels of the target genes (*NFATc1*, *TRAP*, *calcitonin Receptor* (*CTR*) and *cathepsin K* (*CTSK*)) were normalized to that of the reference gene *β-actin*. The $2^{-\Delta\Delta Ct}$ method [29] was used to calculate the relative gene expression. These PCR products were subjected to melting curve analysis and a standard curve to confirm accurate amplification. All PCRs were performed in triplicate, and the primers used for PCR are as follows: *NFATc1*, 5'-CAAGTCTCACCACAGGGCTCACTA-3' (forward), 5'-TCAGCCGTCCCAATGAACAG-3' (reverse); *TRAP*, 5'-CTGGAGTGCACGATGCCAGCGACA-3' (forward), 5'-TCCGTCTCGGCGATGGACCAGA-3' (reverse); *CTR*, 5'-GCTGGAGCCACAGCCTATCA-3' (forward), 5'-CGGTTGCTGTCAGGGTGTCTAA-3' (reverse); *CTSK*, 5'-CACCCAGTGGGAGCTATGGAA-3' (forward), and 5'-GCCTCCAGGTTATGGGCAGA-3' (reverse); *β-actin*, 5'-CATCCGTAAAGACCTCTATGCCAAC-3' (forward), 5'-ATGGAGCCACCGATCCACA-3' (reverse).

Intracellular ROS measurement

After osteoclastic induction for six days, RAW264.7 cells were incubated with serum-free medium containing PrA and/or H_2O_2 for two days. The expression level of intracellular ROS was measured using the ROS assay kit. The relative fluorescence was determined using a multi-detection micro-plate reader with excitation and emission wavelengths of 485 nm and 535 nm, respectively.

Animals and PrA supplementation

All experimental procedures on the animals were performed with official approval from the Medical Ethics Committee of the Lanzhou General Hospital of Lanzhou Military Command (permission code 2016KYLL028). Forty eight-week-old BALB/c female mice (weighing 20-22 g) were randomly chosen. The mice were acclimated to the laboratory environment (a well-ventilated controlled room at 20°C with a 12-h light/dark cycle and free access to water and food) for one week prior to the surgery. The mice were then subjected to a sham operation (n = 10) or surgically ovariectomized (OVX, n = 30) after anesthesia by pentobarbital sodium (50 mg/kg body weight, i.p.). The mice were randomly divided into four groups: untreated (Sham: sham-operated controls), untreated (OVX controls), OVX administered intraperitoneally with PrA (5 mg/kg body weight) daily and OVX administered intraperitoneally with PrA (25

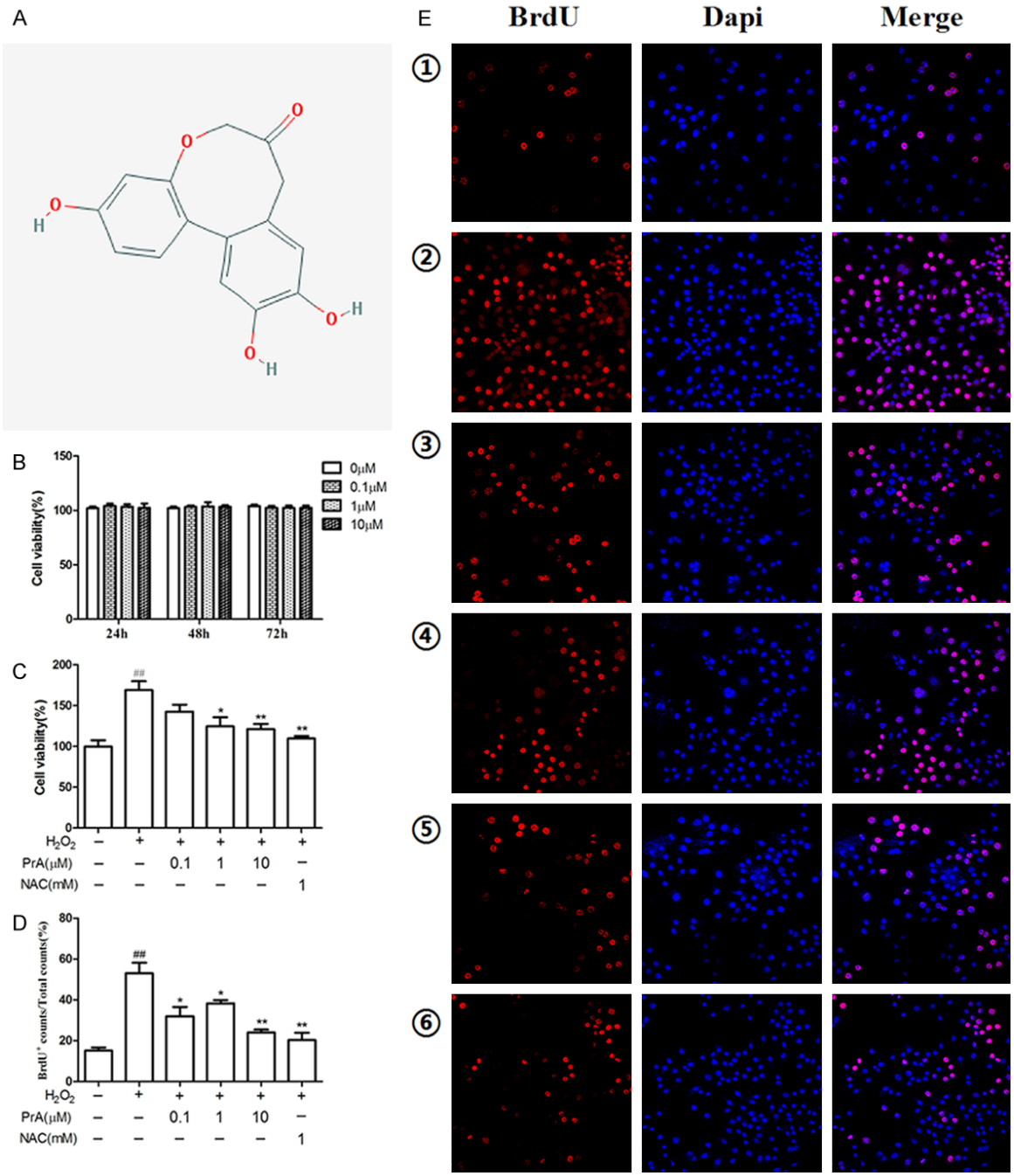

Figure 1. Chemical structure and cytotoxicity of PrA in RAW264.7 cells. A: Chemical structure of PrA. B: RAW264.7 cells were cultured with different concentrations of PrA alone. C: RAW264.7 cells were administered PrA for 24 h and then treated with 0.3 mM H_2O_2 for 24 h. The cell survival of the control RAW264.7 cells was 0.71 ± 0.03 OD. D: Percentage of BrdU-positive cells in each group. E: BrdU staining of RAW264.7 cells. ① Control group; ② H_2O_2; ③ H_2O_2 + PrA (0.1 μM); ④ H_2O_2 + PrA (1 μM); ⑤ H_2O_2 + PrA (10 μM); ⑥ H_2O_2 + NAC (1 mM). ##P < 0.01 compared with the control group; *P < 0.05 and **P < 0.01 compared with the group treated with H_2O_2 alone.

mg/kg body weight) daily. PrA was dissolved in distilled water. Distilled water alone was injected into the untreated controls. One week after the operation, PrA supplementation was initiated and continued for 12 weeks. Blood samples were obtained from the hearts, and the serum was prepared by centrifugation. The left femurs and fourth lumbar vertebrae (L4) of the mice were removed and cleaned of adherent tissues.

Measurements of serum MDA, GSH, CTX-1 and TRAP

MDA is an end-product of lipid peroxidation induced by ROS. GSH is an intracellular antioxidant that protects cells from oxidative stress caused by free radicals, peroxides and toxins [30]. Both MDA and GSH are good oxidative stress markers. The MDA activity in whole-blood samples was determined using the lipid peroxidation MDA assay kit according to the manufacturer's instructions. GSH activity was determined using the GSH assay kit based on the reaction of GSH with 5.50-dithiobis-2-nitrobenzoic acid (DTNB) to produce a product that can be measured using a spectrophotometer at 412 nm. The bone degradation markers CTX-1 and TRAP were tested using ELISA assay kits according to the manufacturer's instructions.

Assessment of bone micro-architecture using micro-CT

The bone micro-architecture of L4 and distal femur was scanned using a Locus SP Pre-Clinical Specimen micro-CT (GE Healthcare, USA) with 8-mm resolution, 50-kV tube voltage and 0.1-mA tube current as previously described [31]. Reconstruction and 3D quantitative analyses were performed using software provided by a desktop micro-CT system (GE Healthcare, USA). The following 3D indices in the defined region of interest (ROI) were analyzed: BMD, trabecular number (Tb.N), trabecular thickness (Tb.Th) and relative bone volume over total volume (BV/TV, %). The operator who performed the scan analysis was blinded to the treatment of the specimens.

Data analysis

All results are expressed as means and S.D. of several independent experiments (n = 5). Multiple comparisons of the data were performed by ANOVA with Dunnett's test. *P* values less than 5% were regarded as significant.

Results

Chemical structure and toxicity of PrA in RAW264.7 cells

The chemical structure of PrA (from the National Center of Biotechnology Information, PubChem CID: 128001) is shown in **Figure 1A**. We tested the survival of RAW264.7 cells to observe the cytotoxic effects of PrA. The data presented in **Figure 1B** show that PrA (0.1, 1, and 10 μM) administration alone had no toxic effects as accessed by cell viability in RAW264.7 cells. However, the treatment of RAW264.7 cells with PrA (0.1, 1, and 10 μM) for one day prior to H_2O_2 treatment significantly decreased the survival of these cells compared with the group treated with H_2O_2 alone, suggesting that PrA promotes H_2O_2-induced RAW264.7 cell apoptosis (**Figure 1C**).

To further evaluate the effect of PrA on RAW264.7 cell proliferation, these cells were treated with BrdU to label the dividing cells. The percentage of BrdU-positive cells for each group was observed and calculated (**Figure 1D** and **1E**). Compared with the control group, H_2O_2 treatment increased the proliferating rate of RAW264.7 cells. However, PrA intervention rescued the up-regulating effect of H_2O_2 (**Figure 1**). Therefore, the results clearly showed that PrA inhibited the H_2O_2-induced proliferation of RAW264.7 cells.

PrA reduced osteoclast activity and differentiation in RAW264.7 cells

We examined the effects of PrA on RAW264.7 activity and differentiation through TRAP staining and bone resorption pit assay. We then measured the mRNA expression of osteoclastic genes. In contrast to the control group, all of the osteoclastic markers, such as TRAP positive staining, osteoclast activity and osteoclastic gene expressions (**Figure 2**), were significantly increased after H_2O_2 treatment. However, the treatment of RAW264.7 cells with PrA (0.1, 1, and 10 μM) resulted in a significant decrease in TRAP-positive cells (**Figure 2A** and **2C**) and osteoclast activity (**Figure 2B** and **2D**). Moreover, pre-treatment with PrA significantly suppressed the mRNA expression of osteoclastic genes in contrast to the group treated with H_2O_2 alone (**Figure 2**). To conclude, these results showed that PrA reduced H_2O_2-induced RAW264.7 activation and differentiation.

PrA inhibited ROS generation in RAW264.7 cells

To elucidate whether the beneficial effects of PrA on cells are associated with its antioxidant

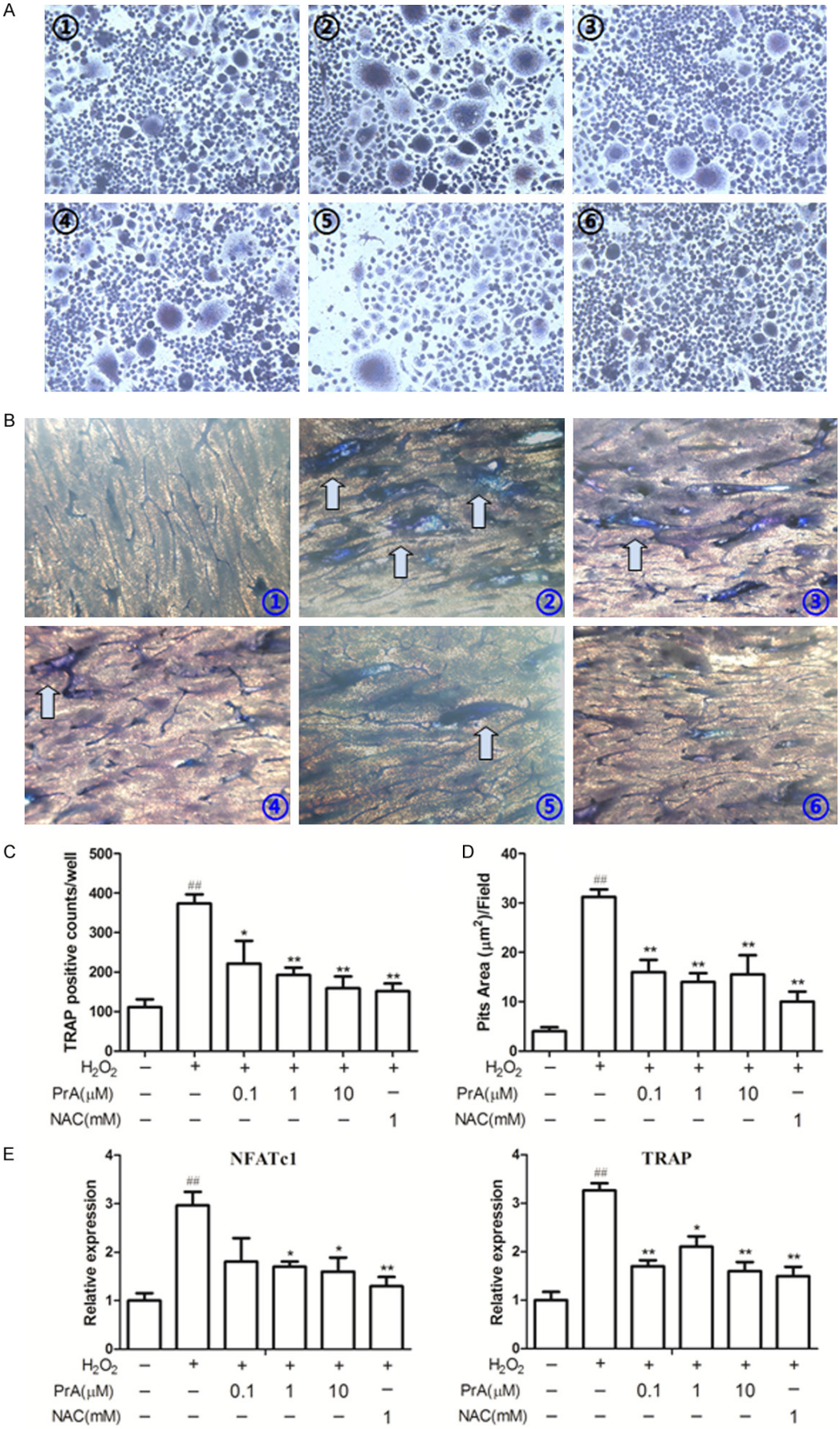
A
B
C
TRAP positive counts/well
D
Pits Area (μm²)/Field
E
NFATc1
TRAP
Relative expression
H2O2
PrA(μM)
NAC(mM)

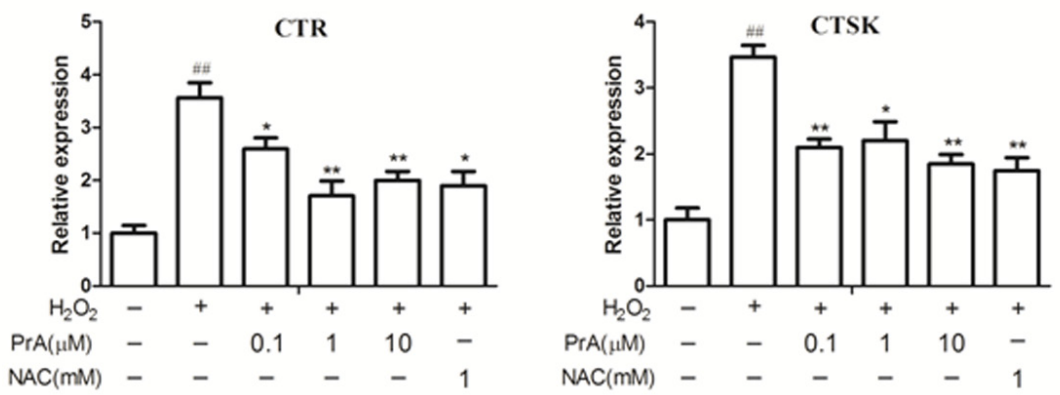

Figure 2. PrA reduced osteoclast activity and differentiation in RAW264.7 cells. A: The cells were stained for TRAP activity. B: Measurement of osteoclast activity by bone resorption pit assay. RAW264.7 cells, which were generated on bone, were removed after six days. The resorptive lacunae were stained by lectin, and the pit area was determined. ① Control group; ② H_2O_2; ③ H_2O_2 + PrA (0.1 μM); ④ H_2O_2 + PrA (1 μM); ⑤ H_2O_2 + PrA (10 μM); ⑥ H_2O_2 + NAC (1 mM). C: Quantification of TRAP-positive cells per well. D: Quantification of osteoclast activity. E: mRNA expression levels of *NFATc1*, *TRAP*, *CTR* and *CTSK* in RAW264.7 cells. ##P < 0.01 compared with the control group; *P < 0.05 and **P < 0.01 compared with the group treated with H_2O_2 alone.

capacity, we tested ROS generation using the fluorescent probe DCFH-DA. The data presented in **Figure 3** show that the treatment of RAW264.7 cells with 300 μM H_2O_2 significantly increased ROS generation. This finding indicated that H_2O_2 stimulated oxidant generation and resulted in oxidative stress in RAW264.7 cells. However, the treatment of the cells with PrA at different concentrations partially suppressed ROS generation (**Figure 3**). These results demonstrated that the beneficial effects of PrA may be associated in part with its antioxidant activity.

PrA suppressed serum oxidative stress and osteoclastic markers in OVX mice

To evaluate the effects of PrA on serum of OVX mice, different concentrations of PrA were administered to mice following an ovariectomy. Then, we measured the MDA, GSH, CTX-1 and TRAP activities in serum. As shown in **Figure 4**, in contrast to the sham-operated group, the OVX group exhibited enhanced MDA, CTX-1 and TRAP activities and reduced GSH activity. However, PrA treatment significantly reduced the serum MDA, CTX-1 and TRAP activities and elevated GSH activity. These results indicated that PrA treatment can partially inhibit the serum oxidative status and the activities of osteoclastic markers.

PrA inhibited osteoclastogenesis in vivo

To evaluate the effects of PrA on the trabecular bone micro-architecture, different concentrations of PrA were administered to mice following an ovariectomy. Analysis of the trabecular bone of L4 and the distal femur demonstrated that OVX deteriorated the trabecular bone micro-architecture, as evaluated by decreases in BMD, Tb.N, Tb.Th and BV/TV (**Figure 5B** and **5C**) compared with the sham-operated group. However, the treatment of OVX mice with 5 or 25 mg/kg PrA ameliorated these adverse effects and improved the trabecular micro-architectures. The amelioration of the bone micro-architecture parameters of distal femurs is shown in the micro-CT images (standard ROI in cylinder type) presented in **Figure 5A**.

Discussion

ROS are produced by various environmental agents as well as by the endogenous oxygen metabolism and are considered to be partly responsible for estrogen deficiency and a number of pathological conditions, such as osteoporosis [32, 33]. Their overproduction induces oxidative damage. Due to its good stability and ability to pass through cell membranes, H_2O_2 likely serves as both an extra- and an inter-cellular signal molecule [34]. Thus, a H_2O_2-induced oxidative stress model was built using RAW264.7 cells in this study. We used a treatment with 300 μM H_2O_2 for 24 h to cause oxidative damage in the present study as previously described [35]. Previous studies have shown that oxidative stress may significantly induce osteoclast precursor proliferation and elevate their functions [35]. Our data showed that pre-

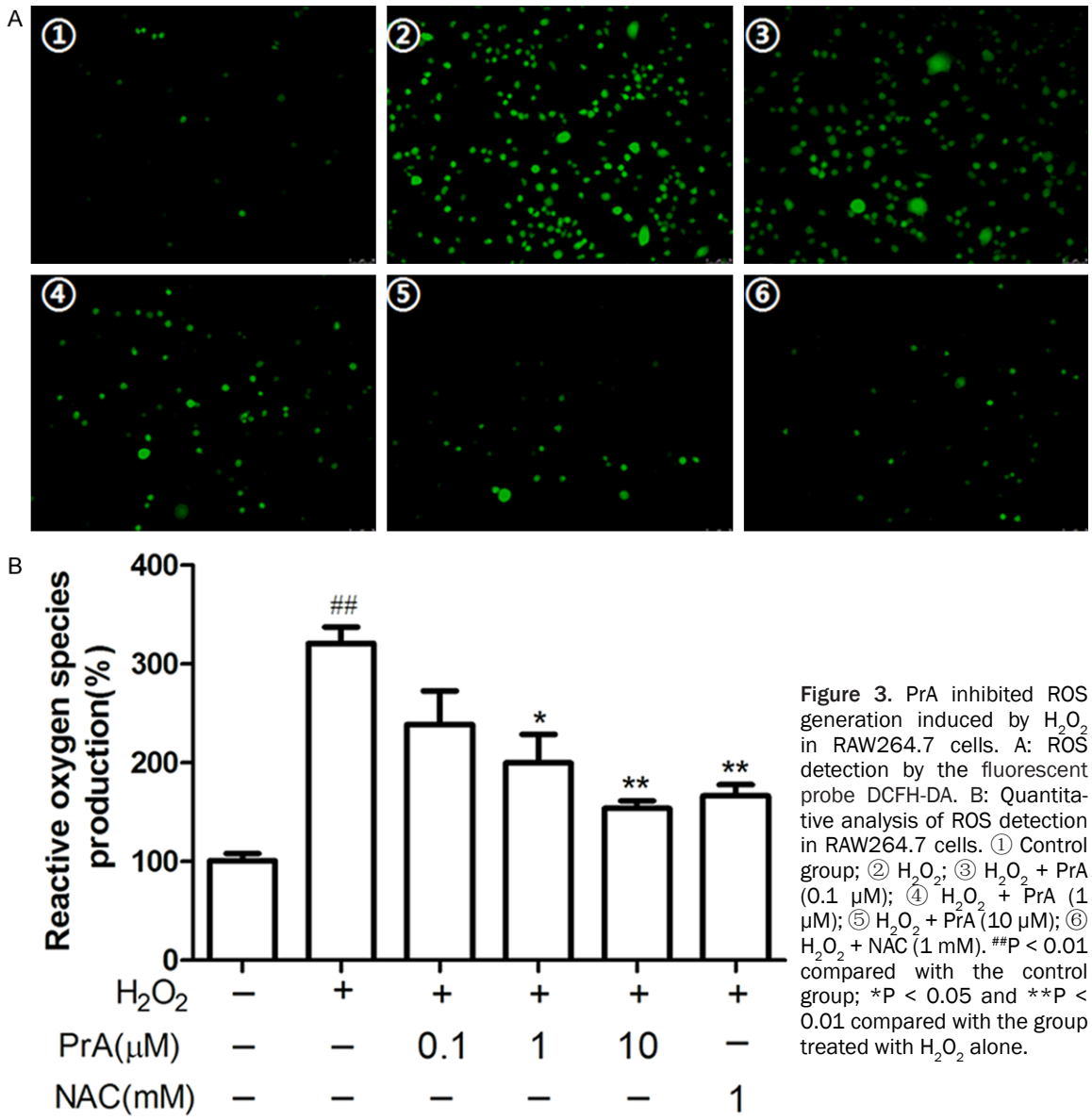

Figure 3. PrA inhibited ROS generation induced by H_2O_2 in RAW264.7 cells. A: ROS detection by the fluorescent probe DCFH-DA. B: Quantitative analysis of ROS detection in RAW264.7 cells. ① Control group; ② H_2O_2; ③ H_2O_2 + PrA (0.1 μM); ④ H_2O_2 + PrA (1 μM); ⑤ H_2O_2 + PrA (10 μM); ⑥ H_2O_2 + NAC (1 mM). $^{\#\#}P < 0.01$ compared with the control group; $^{*}P < 0.05$ and $^{**}P < 0.01$ compared with the group treated with H_2O_2 alone.

treatment with PrA ameliorated the effect of H_2O_2 to some degree. Our study suggested that PrA decreased the H_2O_2-induced proliferation of RAW264.7 cells.

In addition to influencing RAW264.7 cell proliferation, oxidative stress also affects their function and differentiation. It has previously been shown *in vitro* and in rodents that free radicals are involved in osteoclastogenesis and in bone resorption [15]. Osteoclasts are derived from the monocyte/macrophage lineages [36]. Mature osteoclasts are characterized by morphological conversion into large multi-nucleated osteoclastic cells and by the expression of specific markers, such as *TRAP*, *CTSK* and *CTR* [37-40]. Our study also showed that H_2O_2 was correlated with an elevation in cellular TRAP activity, an increase in bone resorption and an elevated generation of osteoclastic genes, including *NFATc1*, *TRAP*, *CTSK* and *CTR*, further confirming previous results that H_2O_2 resulted in osteoclast activation and differentiation. Moreover, our results demonstrated that the H_2O_2-induced activation of osteoclastic development can be partially reversed by PrA treatment. However, PrA alone could not significantly enhance RAW264.7 activation and osteoclastic differentiation at the experimental concentrations. Thus, we speculated that the antioxidant

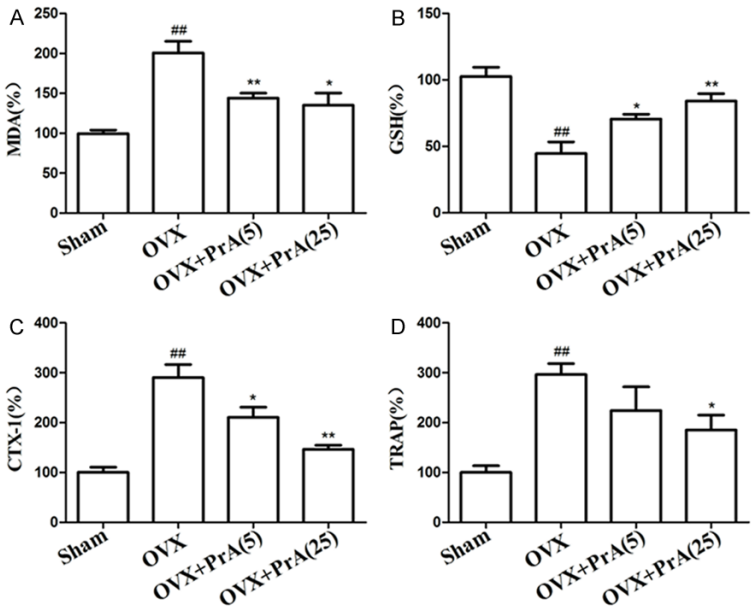

Figure 4. PrA inhibits the oxidative status and osteoclastic markers in serum. A and B: Serum MDA and GSH activities in OVX mice supplemented with different concentrations of PrA. The control values for MDA and GSH were 7.28 ± 0.23 nM/mg and 10.56 ± 0.44 nM/mg. C and D: Serum CTX-1 and TRAP levels in OVX mice supplemented with different concentrations of PrA. The control values for CTX-1 and TRAP were 22.18 ± 0.26 ng/ml and 13.49 ± 0.32 U/ml. Groups: Sham; OVX; OVX + PrA (5 mg/kg); OVX + PrA (25 mg/kg). ##P < 0.01 versus the sham-operated group; *P < 0.05 and **P < 0.01 compared with the OVX group.

activity induced a protective effect of PrA. By inhibiting the differentiation of RAW264.7 cells against oxidative stress, PrA may become an appropriate anti-osteoporosis herbal agent in bone resorption-related fields.

PrA extracted from *Caesalpinia sappan L*. is a novel biphenyl compound. The anti-oxidative property of PrA was recently investigated [23]. In this study, we partially reversed the H_2O_2-induced generation of ROS by treatment with PrA. Our data indicated that PrA may be a useful antioxidant to partially protect RAW264.7 cells against proliferation and differentiation induced by oxidative stress. Consequently, the protection of RAW264.7 cells by PrA may be mediated via its antioxidant capacity. However, the detailed molecular mechanism explaining these effects has not been established. The finding of osteopetrosis in mice lacking NF-κB [41], the discovery of the receptor activator of NF-κB (RANK), the RANK ligand, and the decoy receptor osteoprotegerin demonstrated the great importance of NF-κB in osteoclastogenesis. NF-κB is an oxidative stress-responsive transcription factor [42]. Thus, free radicals may increase bone resorption through NF-κB activation. Wu and his colleagues found that PrA induces immunosuppression of rats heart transplantation targeting T cells in grafts via NF-κB pathway [22]. Under these circumstances, we hypothesized that PrA treatment provided protective effects against activation and differentiation induced by H_2O_2 in RAW264.7 cells, at least partly, via the NF-κB signaling pathway. In further studies, we will attempt to explore this molecular mechanism.

The mechanism through which estrogen deficiency activates bone loss is not fully understood. Oxidative stress was recently shown to result in postmenopausal osteoporosis. It has been reported that the increases in oxidative stress and $p66^{shc}$ phosphorylation observed with age-related changes in the bone of C57BL/6 mice are caused by gonad removal in female or male mice [43]. Moreover, these alterations were ameliorated in gonadectomized animals via the administration of antioxidants, such as NAC, ascorbate and catalase, which are effective as hormone replacements [4]. These antioxidants were given to animals orally or intraperitoneally. Both delivery modes are beneficial under the right circumstances. ICR mice were administered orally with 10 mg/kg PrA solution for 7 days in vivo in Zeng's group [23]. However, we want to explore if PrA functions well intraperitoneally. In our study, we treated BALB/c female mice with PrA for 12 weeks intraperitoneally. Our data showed that PrA partially reversed the serum MDA and GSH activities in OVX mice. The serum CTX-1 and TRAP activities are markers of osteoclast resorption, respectively, and are reportedly increased in OVX animals relative to sham-operated animals [44]. However, PrA treatment significantly reduced their activities in serum. Our results indicated that PrA treatment can inhibit the serum osteoclastic markers in OVX mice.

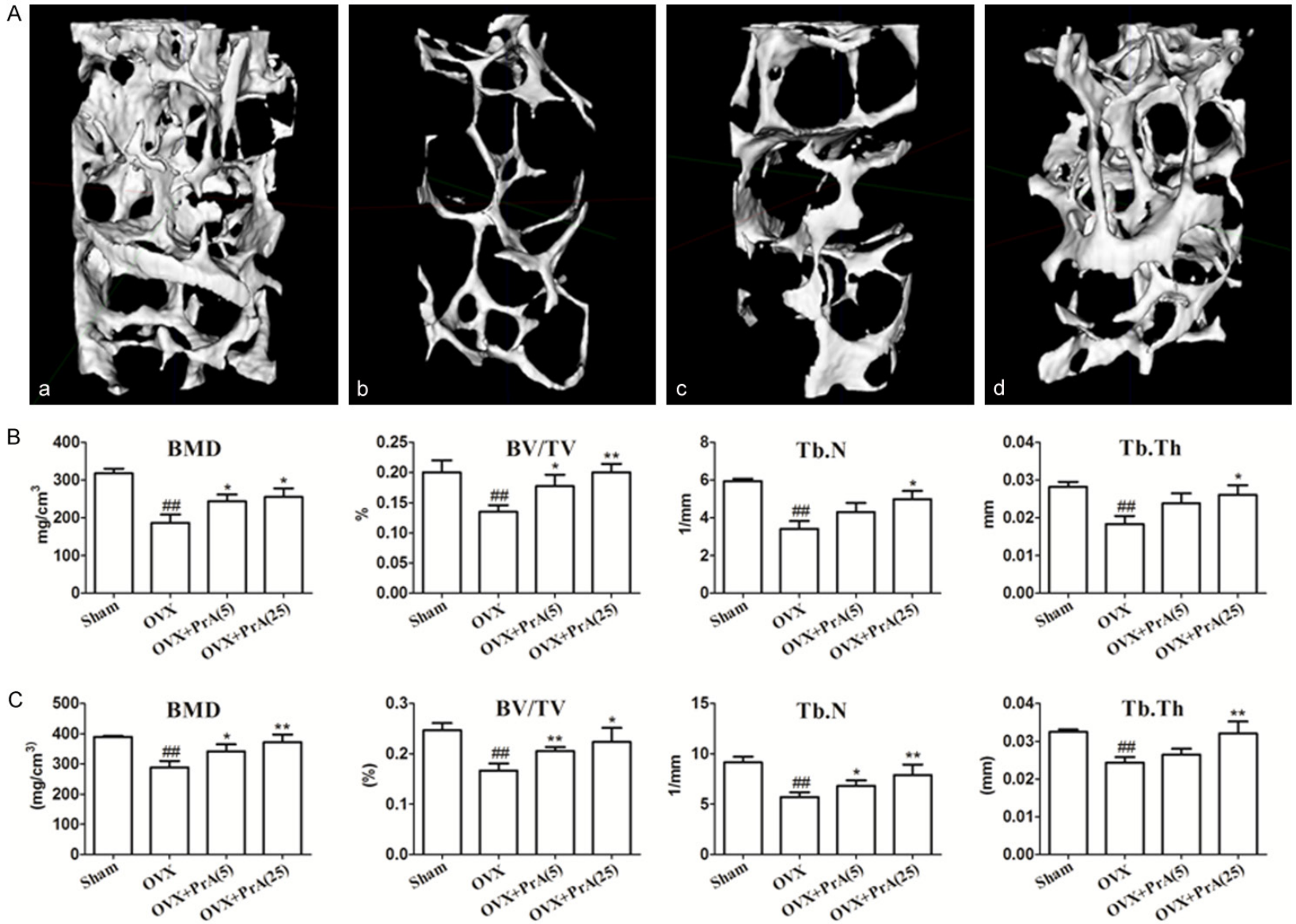

Figure 5. PrA inhibited osteoclastogenesis *in vivo*. A: Micro-CT analysis within the distal metaphyseal femur region (standard ROI in cylinder type). B: Quantification of micro-CT analysis within the distal metaphyseal femur region. C: Quantification of micro-CT analysis within the fourth lumbar vertebrae. The following 3D indices in the defined ROI were analyzed: BMD, Tb.N, Tb.Th and BV/TV. Groups: a: Sham; b: OVX; c: OVX + PrA (5 mg/kg); d: OVX + PrA (25 mg/kg). ##P < 0.01 compared with the sham group; *P < 0.05 and **P < 0.01 compared with the OVX group.

The BMD has been recognized as an important predictor of osteoporosis fractures, but previous studies have reported 10-53% compliance with BMD criteria to diagnose osteoporosis in the presence of osteoporotic fractures [45]. However, a micro-CT voxel-based test unit is able to detect lesions and structures in bone early [46]. The trabecular bone micro-architecture is considered a proper predictor of OVX-induced bone loss and bone structure deterioration [47]. Thus, we examined the trabecular micro-architectures after the administration of PrA using micro-CT scanning. A previous micro-CT analysis showed that the normal trabecular bone micro-architectures are markedly deteriorated after ovariectomy, which is consistent with the results obtained in our research [48]. In addition, ovariectomy can induce osteoclast formation *in vivo*, as determined through TRAP staining. However, pre-treatment with PrA reduced the osteoclast numbers in OVX mice. Taken together, these results suggested that PrA may inhibit osteoclastogenesis in OVX mice and that PrA may represent a good prevention and treatment method for estrogen-deficient osteoporosis.

However, we should note that our research study has some limitations. A detailed study of the molecular mechanisms may strengthen our results. Additionally, the effect of PrA on bone formation has not been fully investigated. We will address these questions in future studies to supplement our current results.

The results described in this study indicated that PrA protects RAW264.7 cells from proliferation and differentiation induced by H_2O_2 *in vitro*, and this effect is accompanied by a decrease in oxidative stress. PrA decreases serum ROS generation and osteoclastic markers. Moreover, PrA partially reverses the effects of ovariectomy and inhibits osteoclastogenesis *in vivo*.

Acknowledgements

This work was supported by the National Natural Science Foundation of China (81600700) and Open Project from State key Laboratory of Military Stomatology (2016KB02).

Disclosure of conflict of interest

None.

Address correspondence to: Qiu-Ming Gao, Lanzhou General Hospital of Lanzhou Military Command, Lanzhou 730050, Gansu, People's Republic of China. Tel: 86-931-8994313; Fax: 86-931-8994313; E-mail: gaoqiuminghq@163.com

References

[1] Berecki-Gisolf J, Spallek M, Hockey R, Dobson A. Height loss in elderly women is preceded by osteoporosis and is associated with digestive problems and urinary incontinence. Osteoporosis Int 2010; 21: 479-485.

[2] Sanchez-Rodriguez MA, Ruiz-Ramos M, Correa-Munoz E, Mendoza-Nunez VM. Oxidative stress as a risk factor for osteoporosis in elderly Mexicans as characterized by antioxidant enzymes. BMC Musculoskelet Disord 2007; 8: 124.

[3] Vasilaki A, Mansouri A, Remmen H, Van der Meulen JH, Larkin L, Richardson AG, McArdle A, Faulkner JA, Jackson MJ. Free radical generation by skeletal muscle of adult and old mice: effect of contractile activity. Aging Cell 2006; 5: 109-117.

[4] Manolagas SC. From estrogen-centric to aging and oxidative stress: a revised perspective of the pathogenesis of osteoporosis. Endocr Rev 2010; 31: 266-300.

[5] Sendur OF, Turan Y, Tastaban E, Serter M. Antioxidant status in patients with osteoporosis: a controlled study. Joint Bone Spine 2009; 76: 514-518.

[6] Ozgocmen S, Kaya H, Fadillioglu E, Aydogan R, Yilmaz Z. Role of antioxidant systems, lipid peroxidation, and nitric oxide in postmenopausal osteoporosis. Mol Cell Biochem 2007; 295: 45-52.

[7] Witko-Sarsat V, Friedlander M, Capeillere-Blandin C, Nguyen-Khoa T, Nguyen AT, Zingraff J, Jungers P, Descamps-Latscha B. Advanced oxidation protein products as a novel marker of oxidative stress in uremia. Kidney Int 1996; 49: 1304.

[8] Muthusami S, Ramachandran I, Muthusamy B, Vasudevan G, Prabhu V, Subramaniam V, Subramaniam V, Jagadeesan A, Narasimhan S. Ovariectomy induces oxidative stress and impairs bone antioxidant system in adult rats. Clin Chim Acta 2005; 360: 81-86.

[9] Manolagas SC. De-fense! De-fense! De-fense: scavenging H202 while making cholesterol. Endocrinology 2008; 149: 3264-3266.

[10] Izawa T, Zou W, Chappel JC, Ashley JW, Feng X, Teitelbaum SL. c-Src links a RANK/avb3 integrin complex to the osteoclast cytoskeleton. Mol Cell Biol 2012; 32: 2943.

[11] Lean JM, Davies JT, Fuller K, Jagger CJ, Kirstein B, Partington GA, Urry ZL, Chambers TJ. A cru-

cial role for thiol antioxidants in estrogen-deficiency bone loss. J Clin Invest 2003; 112: 915-923.
[12] Lean JM, Jagger CJ, Kirstein B, Fuller K, Chambers TJ. Hydrogen peroxide is essential for estrogen-deficiency bone loss and osteoclasts formation. Endocrinology 2005; 146: 728-735.
[13] Lee NK, Choi YG, Baik JY, Han SY, Jeong DW, Bae YS, Kim N, Lee SY. A crucial role for reactive oxygen species in RANKL-induced osteoclast differentiation. Blood 2005; 106: 852-859.
[14] Altindag O, Erel O, Soran N, Celik H, Selek S. Total oxidative/anti-oxidative status and relation to bone mineral density in osteoporosis. Rheumatol Int 2008; 28: 317-321.
[15] Garrett IR, Boyce BF, Oreffo RO, Bonewald L, Poser J, Mundy GR. Oxygen-derived free radicals stimulate osteoclastic bone resorption in rodent bone in vitro and in vivo. J Clin Invest 1990; 85: 632-639.
[16] Manolagas SC, Jilka RL. Bone marrow, cytokines, and bone remodeling. Emerging insights into the pathophysiology of osteoporosis. N Engl J Med 1995; 332: 305-311.
[17] Behl C. Estrogen can protect neurons: modes of action. J Steroids Biochem Mol Biol 2003; 83: 195-197.
[18] Isomura H, Fujie K, Shibata K, Inoue N, Iizuka T, Takebe G, Takahashi K, Nishihira J, Izumi H, Sakamoto W. Bone metabolism and oxidative stress in postmenopausal rats with iron overload. Toxicology 2004; 197: 93-100.
[19] Eslami B, Zhou S, Van Eekeren I, LeBoff MS, Glowacki J. Reduced osteoclastogenesis and RANKL expression in marrow from women taking alendronate. Calcif Tissue Int 2011; 88: 272-280.
[20] Turgeon RD, Yeung SS. Fracture risk and zoledronic acid in men with osteoporosis. N Engl J Med 2012; 367: 1714-1723.
[21] Soda T, Fukumoto R, Hayashi T, Oka D, Fujimoto N, Koide T. A case of prostate cancer associated with bisphosphonate-related osteonecrosis of the jaw followed by retropharyngeal abscess. Hinyokika Kiyo 2013; 59: 587-591.
[22] Wu J, Zhang MM, Jia HB, Huang XT, Zhang Q, Hou JB, Bo Y. Protosappanin A induces immunosuppression of rats heart transplantation targeting T cells in grafts via NF-κB pathway. Naunyn-Schmied Arch Pharmacol 2010; 381: 83-92.
[23] Zeng KW, Zhao MB, Ma ZZ, Jiang Y, Tu PF. Protosappanin A inhibits oxidative and nitrative stress via interfering the interaction of transmembrane protein CD14 with Toll-like receptor-4 in lipopolysaccharide-induced BV-2 microglia. Int Immunopharmacol 2012; 14: 558-569.
[24] Sasaki Y, Hosokawa T, Nagai M, Nagumo S. In vitro study for inhibition of NO production about constituents of Sappan Lignum. Biol Pharm Bull 2007; 30: 193-6.
[25] Sharma P, Patntirapong S, Hann S, Hauschka PV. RANKL-RANK signaling regulates expression of xenotropic and polytropic virus receptor (XPR1) in osteoclasts. Biochem Biophys Res Commun 2010; 399: 129-32.
[26] Chiang HM, Chen HC, Lin TJ, Shih IJ, Wen KC. Michelia alba extract attenuates UVB-induced expression of matrix metalloproteinases via MAP kinase pathway in human dermal fibroblast. Food Chem Toxicol 2012; 50: 4250-4269.
[27] Izawa T, Zou W, Chappel JC, Ashley JW, Feng X, Teitelbaum SL. c-Src links a RANK/avb3 integrin complex to the osteoclast cytoskeleton. Mol Cell Biol 2012; 32: 2943.
[28] Zhang JK, Yang L, Meng GL, Fan J, Chen JZ, He QZ, Chen S, Fan JZ, Luo ZJ, Liu J. Protective effect of tetrahydroxystilbene glucoside against hydrogen peroxide-induced dysfunction and oxidative stress in osteoblastic MC3T3-E1cells. Eur J Pharmacol 2012; 689: 31-37.
[29] Livak KJ, Schmittgen TD. Analysis of relative gene expression data using real-time quantitative PCR and the 2-ΔΔCT method. Methods 2001; 25: 402-408.
[30] Estrela JM, Ortega A, Obrador E. Glutathione in cancer biology and therapy. Crit Rev Clin Lab Sci 2006; 43: 143-181.
[31] Zhang JK, Yang L, Meng GL, Yuan Z, Fan J, Li D, Chen JZ, Shi TY, Hu HM, Wei, BY, Luo ZJ, Liu J. Protection by salidroside against bone loss via inhibition of oxidative stress and bone-resorbing mediators. PLoS One 2013; 8: e57251.
[32] Baek KH, Oh KW, Lee WY, Lee SS, Kim MK, Kwon HS, Rhee EJ, Han JH, Song KH, Cha BY, Lee KW, Kang M. Association of oxidative stresswith postmenopausal osteoporosis and the effects of hydrogen peroxide on osteoclast formation in human bone marrow cell cultures. Calcif Tissue Int 2010; 87: 226-235.
[33] Basu S, Michaelsson K, Olofsson H, Johansson S, Melhus H. Association between oxidative stress and bone mineral density. Biochem Biophys Res Commun 2001; 288: 275-279.
[34] Denisova NA, Cantuti-Castelvetri I, HaRb2n WN, Paulson KE, Joseph JA. Role of membrane lipids in regulation of vulnerability to oxidative stress in PC12 cells: implication for aging. Free Radic Biol Med 2001; 30: 671-678.
[35] Bax BE, Alam AS, Banerji B, Bax CM, Bevis PJ, Stevens CR, Moonga BS, Blake DR, Zaidi M. Stimulation of osteoclastic bone resorption by hydrogen peroxide. Biochem Biophys Res Commun 1992; 183: 1153-1158.
[36] Mohamed SG, Sugiyama E, Shinoda K, Taki H, Hounoki H, Abdel-Aziz HO, Maruyama M, Ko-

bayashi M, Ogawa H, Miyahara T. Interleukin-10 inhibits RANKL-mediated expression of NFATc1 in part via suppression of c-Fos and c-Jun in RAW264. 7 cells and mouse bone marrow cells. Bone 2007; 41: 592-602.

[37] Anusaksathien O, Laplace C, Li X, Ren Y, Peng L, Goldring SR, Galson DL. Tissue-specific and ubiquitous promoters direct the expression of alternatively spliced transcripts from the calcitonin receptor gene. J Biol Chem 2001; 276: 22663-22674.

[38] Motyckova G, Weilbaecher K, Horstmann M, Rieman D, Fisher D. Linking osteopetrosis and pycnodysostosis: regulation of cathepsin K expression by the microphthalmia transcription factor family. Proc Natl Acad Sci U S A 2001; 98: 5798-5803.

[39] Reddy S, Hundley J, Windle J, Alcantara O, Linn R, Leach R, Boldt DH, Roodman GD. Characterization of the mouse tartrate-resistant acid phosphatase (trap) gene promoter. J Bone Miner Res 1995; 10: 601-606.

[40] Choi HJ, Park YR, Nepal M, Choi BY, Cho NP, Choi SH, Heo SR, Kim HS, Yang MS, Soh Y. Inhibition of osteoclastogenic differentiation by Ikarisoside A in RAW 264.7 cells via JNK and NF-jB signaling pathways. Eur J Pharmacol 2010; 636: 28-35.

[41] Iotsova V, Caamano J, Loy J, Yang Y, Lewin A, Bravo R. Osteopetrosis in mice lacking NF-kappaB1 and NFkappaB2. Nat Med 1997; 3: 1285-1289.

[42] Schreck R, Rieber P, Baeuerle PA. Reactive oxygen intermediates as apparently widely used messengers in the activation of the NF-kappa B transcription factor and HIV-1. EMBO J 1991; 10: 2247-2258.

[43] Almeida M, Han L, Martin-Millan M, Plotkin LI, Stewart SA, Roberson PK, Kousteni S, O'Brien CA, Bellido T, Parfitt AM, Weinstein RS, Jilka RL, Manolagas SC. Skeletal involution by age-associated oxidative stress and its acceleration by loss of sex steroids. J Biol Chem 2007; 282: 27285-27297.

[44] Yoon KH, Cho DC, Yu SH, Kim KT, Jeon Y, Sung JK. The change of bone metabolism in ovariectomized rats: analyses of microCT scan and biochemical markers of bone turnover. J Korean Neurosurg Soc 2012; 51: 323-327.

[45] McNamara LM. Perspective on post-menopausal osteoporosis: establishing an interdisciplinary understanding of the sequence of events from the molecular level to whole bone fractures. J R Soc Interface 2010; 7: 353-372.

[46] Boyd SK, Davison P, Müller R, Gasser JA. Monitoring individual morphological changes over time in ovariectomized rats by in vivo micro-computed tomography. Bone 2006; 39: 854-862.

[47] Chappard D, Basle MF, Legrand E, Audran M. Trabecular bone microarchitecture: a review. Morphologie 2008; 92: 162-170.

[48] Ferreri SL, Talish R, Trandafir T, Qin YX. Mitigation of bone losswith ultrasound induced dynamic mechanical signals in an OVX induced rat model of osteopenia. Bone 2011; 48: 1095-1102.